Molecular dynamics investigation of thickness effect on liquid films

Jian-Gang Weng, Seungho Park,[a] Jennifer R. Lukes, and Chang-Lin Tien[b]
Department of Mechanical Engineering, University of California, Berkeley, California 94720-1740

(Received 19 April 2000; accepted 14 July 2000)

This work applies the molecular dynamics simulation method to study a Lennard-Jones liquid thin film suspended in the vapor and to explore the film thickness effect on its stability. For the accurate estimation of local pressure distributions in the film, an improved method is proposed and used. Simulation results indicate that profiles of the local surface tension distribution vary widely with film thickness, while surface tension values and density profiles show little variation. As the film gets thinner, the two liquid–vapor interfacial regions begin to overlap and liquid-phase molecules in the center region of the film experience larger tension in the direction parallel to the film surface. Such interface overlapping is believed to destabilize the film and the occurrence of film rupture depends on the system temperature and the cross-sectional area of the computational domain. © *2000 American Institute of Physics.* [S0021-9606(00)70138-3]

I. INTRODUCTION

The liquid–vapor interface has been subject to extensive study for more than one century because of its critical importance in many industrial applications such as phase-change heat transfer, spread wetting, and material processing. The thickness of an interfacial region is in the nanometer range, making experimental studies of such a thin region extremely difficult. Although there exist a few experimental works on the liquid–vapor interface,[1] physical understanding of interfacial phenomena still relies heavily on theoretical analysis and numerical simulations. Molecular Dynamics (MD) simulation is one of the most effective tools to study interfacial phenomena since it can yield detailed information on the molecular structure of an interface if the appropriate intermolecular potential is given.

The past 10 years have seen a number of reported MD simulations on three-dimensional planar liquid–vapor interfaces after the pioneering work by Chapela *et al.*[2] Specifically, Nijmeijer *et al.*[3] and Daiguji and Hihara[4] calculated the local surface tension of a liquid film sandwiched by its vapor. Mecke *et al.*[5] investigated the influence of the cut-off radius on interfacial properties and proposed a new long-range force correction method. Hwang *et al.*[6] applied MD simulations to observe the transient evolution of rupture processes of a free liquid film and a film on a solid substrate. Despite the increasing practical importance of thin liquid films, however, the effect of liquid film thickness on interfacial properties, such as density, surface tension, and local pressures, has not been reported.

The object of this work, therefore, is to investigate the film thickness effect on the liquid–vapor interface. The interfacial property simulation techniques are very similar to those adopted in the previous MD studies[3–5] except that an improved method is developed in order to obtain a better estimation of the local surface tension profile across the film. The film stability analysis then follows in which results from classical thermodynamic theory and MD simulation are qualitatively compared. Both results indicate that the film thickness has a significant effect on film stability.

II. SIMULATION TECHNIQUE

This simulation uses the well-known Lennard-Jones (LJ) 12-6 potential, given as

$$\phi(r_{ij})=4\varepsilon[(\sigma/r_{ij})^{12}-(\sigma/r_{ij})^{6}]. \tag{1}$$

For the ease of physical understanding, the LJ fluid is assumed to be argon, and parameters for argon are listed as follows:[7] the length parameter $\sigma=0.34$ nm, the energy parameter $\varepsilon=1.67\times10^{-21}$ J, and the molecular mass $m=6.63\times10^{-26}$ kg. The cut-off radius r_c beyond which the intermolecular interaction is neglected is 5.0σ. Separate runs with $r_c=6.5\sigma$ are carried out and the results in both surface tension values and local stress profiles (discussed in Sec. IV) are very close to those with $r_c=5.0\sigma$, which indicates that the cut-off radius at 5.0σ is large enough. The long-range force correction is not used in this preliminary study since the error introduced by neglecting long-range forces is about 10% for this cut-off radius.[5]

The simulation domain is schematically shown in Fig. 1, with periodic boundary conditions applied in all three directions. Simulation domain dimensions, system temperatures T^*, and initial film thicknesses L_s^* are listed in Table I together with simulation results of equilibrated film thickness L_f^* and surface tension γ^*. The equations of motion are solved by using the ''velocity Verlet'' algorithm[7] with a time step of 5 fs, or $\Delta\tau^*=2.335\times10^{-3}$. Note that in this work, all quantities with an asterisk, such as ρ^* and γ^*, are nondimensionalized according to σ, ε, and m.

At the beginning of the simulation, a liquid sheet of initial thickness L_s^* is placed at the center of the computational domain and its two sides are filled with vapor molecules. The initial density of the liquid sheet is 0.8, which is

[a]Also at Department of Mechanical Engineering, Hongik University, Seoul 121-791, Korea.
[b]Author to whom correspondence should be addressed.

 © 2000 American Institute of Physics

Downloaded 04 Sep 2005 to 165.123.34.86. Redistribution subject to AIP license or copyright, see http://jcp.aip.org/jcp/copyright.jsp

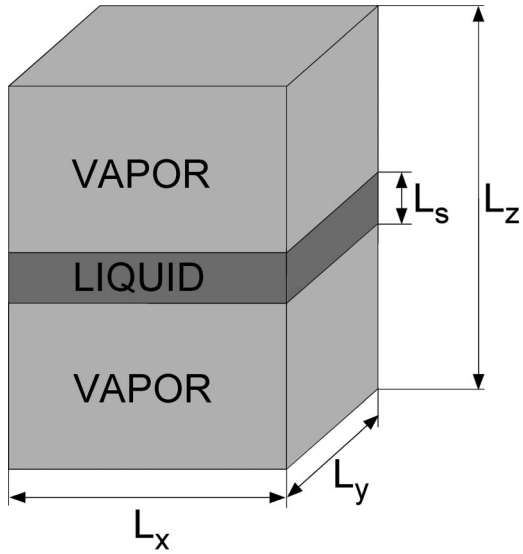

FIG. 1. System configuration for a thin film in its vapor.

slightly higher than the experimental value of saturated bulk liquid argon (e.g., 0.776 at $T^*=0.818$).[8] In contrast, the vapor density, 0.008, is slightly lower than the experimental saturated vapor argon density (0.009 25 at that temperature).[8] The vapor and liquid molecules have been equilibrated individually for 80 000 time steps at the designed temperature T^* before they are put together into the computational domain. The computational domain is artificially divided into many thin slabs in the direction normal to the film surface (z direction) with the slab thickness L_{sl}^* equal to 0.1. Time-averaged values of the density and pressure in each slab are considered as local values. In the simulation, the equilibration period of 40 000 time steps, in which velocity rescaling is performed at each step, is to make sure that the system is at the designed temperature, followed by a relaxation period of another 40 000 time steps. Then the production period of 80 000 time steps starts, in which instantaneous values of the local density and stress are calculated at each time step and time-averaged values are obtained at the end of this period.

III. DENSITY PROFILES AND SURFACE TENSION

It is of vital importance that the system be at equilibrium before statistical values of the local density and pressure are taken. Due to current computation capacity limitations, the MD method cannot simulate a macroscopically long period. Some criteria have to be chosen to determine whether the system is at equilibrium, but unfortunately, such choices in the literature are still arbitrary. Here, the system is considered to be at equilibrium when the local temperature and normal pressure in each slab are constant. During the production period, the kinetic energy of molecules in each slab is measured and the average values in each slab indicate that the temperature is almost the same throughout the system. The mechanical equilibrium requirement that the normal pressure in each slab should be uniform is also satisfied and will be discussed in the next section.

TABLE I. Simulation conditions and some simulation results. "–" indicates that film rupture occurs.

	Simulation conditions		Film thickness		
Label	$L_x^*\times L_y^*\times L_z^*$	T^*	L_s^* (initial)	L_f^* (final)	γ^*
S1	17.10×17.10×49.59	0.818	8.55	9.00	0.76
S2	17.10×17.10×47.88	0.818	6.84	7.19	0.80
S3	17.10×17.10×46.17	0.818	5.13	5.44	0.78
S4	17.10×17.10×45.74	0.818	4.70	5.03	0.78
S5	17.10×17.10×45.31	0.818	4.28	–	–
H1	17.10×17.10×47.03	0.850	5.99	6.16	0.71
H2	17.10×17.10×46.17	0.850	5.13	–	–
L1	20.26×20.26×46.17	0.818	5.13	5.43	0.76
L2	20.26×20.26×45.74	0.818	4.70	–	–

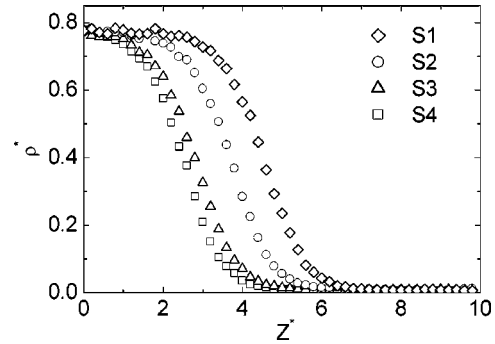

FIG. 2. Density profiles for $L_s^*=8.55$ (S1), $L_s^*=6.84$ (S2), $L_s^*=5.13$ (S3), and $L_s^*=4.70$ (S4) at $T^*=0.818$.

Simulated density profiles in cases (S1–S4) are shown in Fig. 2, where $Z^*=0$ corresponds to the center of the film. The vapor densities ρ_v^* in these cases are about 0.01, and the liquid densities at the film center ρ_l^* vary around 0.775, both of which are close to their counterparts as the bulk saturated densities. The apparent film thickness is determined as the distance between the two equimolar dividing surfaces in the two interfacial regions. The equimolar dividing surface is defined as the surface on which the local density is $0.5(\rho_v^*+\rho_l^*)$. Simulation results of film thickness are shown in Table I as well as the corresponding surface tension values. In some runs (S5, H2, and L2), film rupture occurs and local density profiles and surface tension values cannot be estimated.

The surface tension is calculated by the virial expression[5]

$$\gamma=\frac{1}{4A}\left\langle \sum_{\substack{i<j\\ r_{ij}<r_c}} \left(r_{ij}-\frac{3z_{ij}^2}{r_{ij}}\right)\phi'(r_{ij})\right\rangle, \tag{2}$$

where $A=L_xL_y$ and the angle brackets refer to a time average. The intermolecular distance between two molecules i and j is r_{ij} and its components in each direction are denoted as x_{ij}, y_{ij}, and z_{ij}, respectively. The derivative of LJ potential with respect to r_{ij} is ϕ'. Two conclusions can be drawn from the comparison of surface tension values in Table I. One conclusion is that at the same temperature, the surface tension values vary only slightly with film thickness, with an average value of 0.78 at $T^*=0.818$ that is consistent with the result in the previous work.[5] The other is that the average surface tension value is about 12% higher than the

Downloaded 04 Sep 2005 to 165.123.34.86. Redistribution subject to AIP license or copyright, see http://jcp.aip.org/jcp/copyright.jsp

experimental value (about 9.9 mN/m) for argon at that temperature, corresponding to 0.69 in a nondimensional system). There are several reasons for this deviation, such as neglecting many-body interaction in the LJ potential, neglecting the long-range force correction,[5] and neglecting the finite size effect of the cross-sectional area in the computational domain.[9]

IV. LOCAL STRESS PROFILES

Local stress (also understood as local surface tension[3,4]) is defined as the difference between the local normal and tangential pressure components. Nijmeijer *et al.*[3] and Daiguji and Hihara[4] calculated the local stress distribution across the thin film. In their works, the local normal pressure component p_N and tangential pressure component p_T are expressed as

$$p_N(k)=\langle n(k)\rangle k_B T-\frac{1}{V_{\mathrm{sl}}}\left\langle \sum_{i,j}^{k} \frac{z_{ij}^2}{r_{ij}}\phi'(r_{ij})\right\rangle = p_{N,K}-p_{N,I}, \tag{3}$$

$$p_T(k)=\langle n(k)\rangle k_B T-\frac{1}{V_{\mathrm{sl}}}\left\langle \sum_{i,j}^{k} \frac{\frac{1}{2}(x_{ij}^2+y_{ij}^2)}{r_{ij}}\phi'(r_{ij})\right\rangle = p_{T,K}-p_{T,I}, \tag{4}$$

where $n(k)$ is the number density in slab k, V_{sl} is the volume of slab k ($V_{\mathrm{sl}}=L_x L_y L_{\mathrm{sl}}$) and L_{sl} is the slab thickness. The first terms in Eqs. (3) and (4), $p_{N,K}$ and $p_{T,K}$, are the contribution from kinetic motion of molecules, while the second terms, $p_{N,I}$ and $p_{T,I}$, are the contribution from the intermolecular force. The summation $\Sigma_{i,j}^{k}$ runs over all particle pairs (i,j), of which at least one of the particles is situated in slab k. If only one particle is in slab k, half of the intermolecular force contribution is given to slab k, while the total contribution is given to slab k if both molecules are in that slab. The contribution of pair (i,j) is $z_{ij}^2\phi'(r_{ij})/r_{ij}$ for p_N and $(x_{ij}^2+y_{ij}^2)\phi'(r_{ij})/(2r_{ij})$ for p_T. The surface tension can be expressed as

$$\gamma=\frac{1}{2}\int_0^{L_z}(p_N-p_T)dz, \tag{5}$$

where p_N and p_T refer to the local values. One can prove that Eq. (5) is just another form of Eq. (2).

It should be noted that this is a simplified approach to calculate the local pressure components and is adopted mainly for computational efficiency.[3,4] If detailed information on local pressure components is needed, a more accurate method should be developed. According to Kirkwood and Buff's theory, the intermolecular force contribution to the local normal pressure component is given as the sum over the normal components of all the pair forces acting across a surface element divided by the surface area.[10] The same argument is applicable for the tangential pressure component. In other words, an intermolecular force contributes to local pressure in each plane between the two molecules. Here, the intermolecular force is assumed to act in a straight line. Since in MD simulation of local pressure in a planar interface, a volumetric average is preferred, as can been seen in

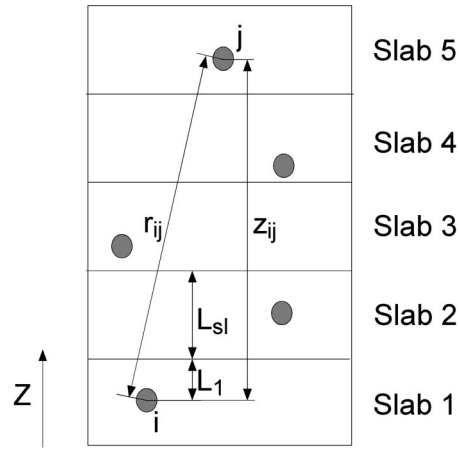

FIG. 3. Schematic pressure combination of the pair *i*, *j*.

Eqs. (3) and (4), Kirkwood and Buff's local pressure tensor is averaged over a distance L_{sl}. All of these form the physical basis for an improved method to calculated local pressure profiles. The whole procedure for the normal pressure component can be expressed as

$$\begin{aligned} p_{N,I}(k) &= \frac{1}{L_{\mathrm{sl}}}\int_{\mathrm{slab_}k}\frac{1}{A}\sum_{i,j}(F_{zij})dz \\ &= \frac{1}{V_{\mathrm{sl}}}\sum_{i,j}\int_{\mathrm{slab_}k}F_{zij}dz \\ &= \frac{1}{V_{\mathrm{sl}}}\sum_{i,j}^{k}F_{zij}L_{k,ij} \\ &= \frac{1}{V_{\mathrm{sl}}}\sum_{i,j}^{k}F_{zij}|z_{ij}|f_{k,ij}, \end{aligned} \tag{6}$$

where F_{zij} is the normal component of the intermolecular force between molecules i and j and the factor $f_{k,ij}$ is defined as $L_{k,ij}/|z_{ij}|$. The third step in the derivation is due to the fact that $F_{zij}$is constant along the line connecting molecules i and j. The length $L_{k,ij}$ is defined as the size of the interval in which F_{zij} is effective in the slab k. For example, consider the force between the pair (i, j) in Fig. 3. If neither molecules is in a slab, such as slab 2, $L_{2,ij}=L_{\mathrm{sl}}$; if one molecule is in a slab, such as slab 1, $L_{1,ij}=L_1$; and if both molecules are in a slab (not shown in Fig. 3), $L_{k,ij}=|z_{ij}|$.

According to this change, the pressure tensor is modified as

$$p_N(k)=\langle n(k)\rangle k_B T-\frac{1}{V_{\mathrm{sl}}}\left\langle \sum_{i,j}^{k}\left(\frac{z_{ij}^2}{r_{ij}}\phi'(r_{ij})f_{k,ij}\right)\right\rangle, \tag{7}$$

$$p_T(k)=\langle n(k)\rangle k_B T - \frac{1}{V_{\mathrm{sl}}}\left\langle \sum_{i,j}^{k}\left(\frac{\frac{1}{2}(x_{ij}^2+y_{ij}^2)}{r_{ij}}\phi'(r_{ij})f_{k,ij}\right)\right\rangle. \tag{8}$$

It should be noted that these two methods yield exactly the same value of surface tension,[3,4] since after substituting Eqs. (7) and (8) to Eq. (5) the integral of $f_{k,ij}$ always gives one. In the bulk liquid with uniform density, these two methods are expected to yield statistically the same results, too.[3,4]

Downloaded 04 Sep 2005 to 165.123.34.86. Redistribution subject to AIP license or copyright, see http://jcp.aip.org/jcp/copyright.jsp

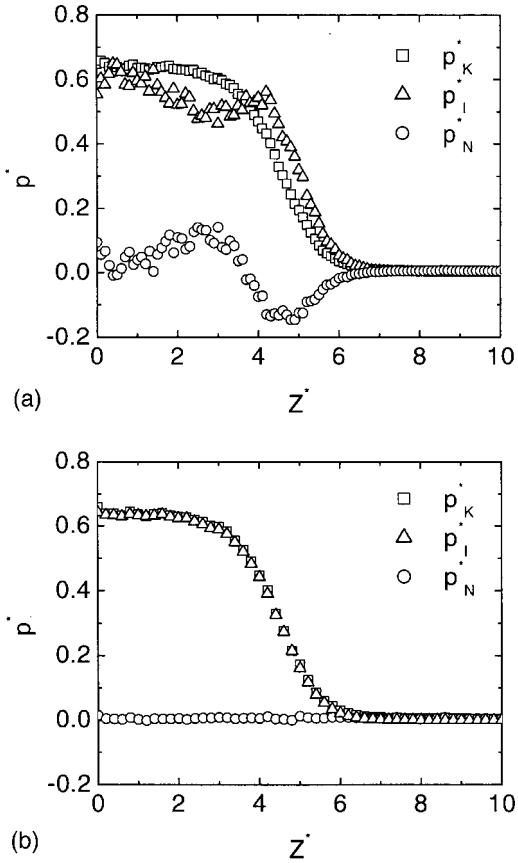

FIG. 4. Normal pressure components calculated from (a) the simplified method and (b) the improved method at $T^*=0.818$ and $L_s^*=8.55$.

However, in an interfacial region, the local stress profiles calculated by these two methods are quite different. As a demonstration, Fig. 4 shows profiles of the normal pressure component for case S1. It is found that p_N^* calculated from the simplified method has significant fluctuation across the interface while the fluctuation disappears in the improved method. Although such fluctuation in the simplified method might be averaged out in a simulation with enough long time, it is quite clear that the improved method can make better estimation of the local pressure. As stated in the previous section, the requirement of mechanical equilibrium is satisfied because the normal pressure does not change significantly.

Figure 5 plots profiles of local values of pressure components $p_{N,I}^*$, $p_{T,I}^*$, and stress $(p_N^*-p_T^*)$ using both simplified and improved methods. It is found that although the surface tension values show little variation with the change of film thickness, the stress distributions are quite different. When the film becomes thinner and thinner, the two interfaces start to interact with each other and the local stress at the center rises, which causes the center liquid to be under the metastable condition.

V. FILM STABILITY

As the film thickness decreases further (S5), film rupture occurs. Figure 6 shows the initial and final position of molecules in the computational domain. From the snapshot of the final molecule position, it is obvious that the film has broken. This indicates that at the given temperature and domain size, the liquid film with the equilibrium thickness L_f^* less than 5.03 is unstable.

Similarly, increasing the temperature T^* or cross-sectional area A $(A=L_xL_y)$ will destabilize the film. As indicated in Table I, when T^* increases to 0.85, the film that is stable at $T^*=0.818$ (S3) becomes unstable (H2); while as L_x^* and L_y^* increase from 17.1 to 20.26, the minimum stable film thickness changes from 5.03 (S4) to 5.43 (L1).

It should be emphasized that although a film is stable in the simulation period of 160 000 time steps (corresponding to 800 ps), that duration is still too short to guarantee against the occurrence of film rupture at some later time. In this sense, what is compared in this work is the ''relative stability'' of the film within a very short period. According to the three simulations above, the minimum thickness of the stable film depends on both the computational domain size and system temperature.

Classically, surface wave theory is applied to study the stability problem of liquid films and cylinders. Many macroscopic models have been developed to study stability of a liquid film on a solid substrate[11,12] and a similar model is now proposed to study the free film stability. Consider the most unstable case in which two synchronic one-dimensional waves propagate along the x direction at each liquid–vapor interface (the ''squeezing'' mode[11]), as shown in Fig. 7. Assume the surface wave can be expressed as a sine wave with wavelength λ and amplitude ΔL. The ''average'' film thickness is L_f. With the assumption that the curvature dependence of surface tension is neglected, the change in total surface energy due to this wave is

$$\Delta W_s=\frac{2\gamma_{lv}(\Delta L\pi)^2}{\lambda}. \tag{9}$$

Note the surface energy change is positive due to the increased surface area. The volumetric energy density in the film can be written as[12]

$$W_{\mathrm{vdw}}=-\frac{A}{12\pi L_f^2}, \tag{10}$$

where A is the Hamaker constant. The volumetric energy change due to this wave is

$$\Delta W_v=\lambda\Delta L^2\left(-\frac{A}{2\pi L_f^4}\right). \tag{11}$$

The volumetric energy change is negative because A is always positive for two identical media (vapor in this case) interacting across another medium (liquid film)[13]. The Hamaker constant can be expressed as[13]

$$A=\frac{3}{4}k_BT\left(\frac{\varepsilon_1-\varepsilon_2}{\varepsilon_1+\varepsilon_2}\right)^2+\frac{3h\nu_e}{16\sqrt{2}}\frac{(n_1^2-n_2^2)^2}{(n_1^2+n_2^2)^{3/2}}, \tag{12}$$

where ε (it is different from the energy parameter in the LJ potential) is the dielectric constant, n the refractive index, h Planck's constant, v_e the main electronic absorption frequency, and the subscripts 1 and 2 refer to the vapor and liquid, respectively. For the vapor phase, ε_1 and n_1 are close

Downloaded 04 Sep 2005 to 165.123.34.86. Redistribution subject to AIP license or copyright, see http://jcp.aip.org/jcp/copyright.jsp

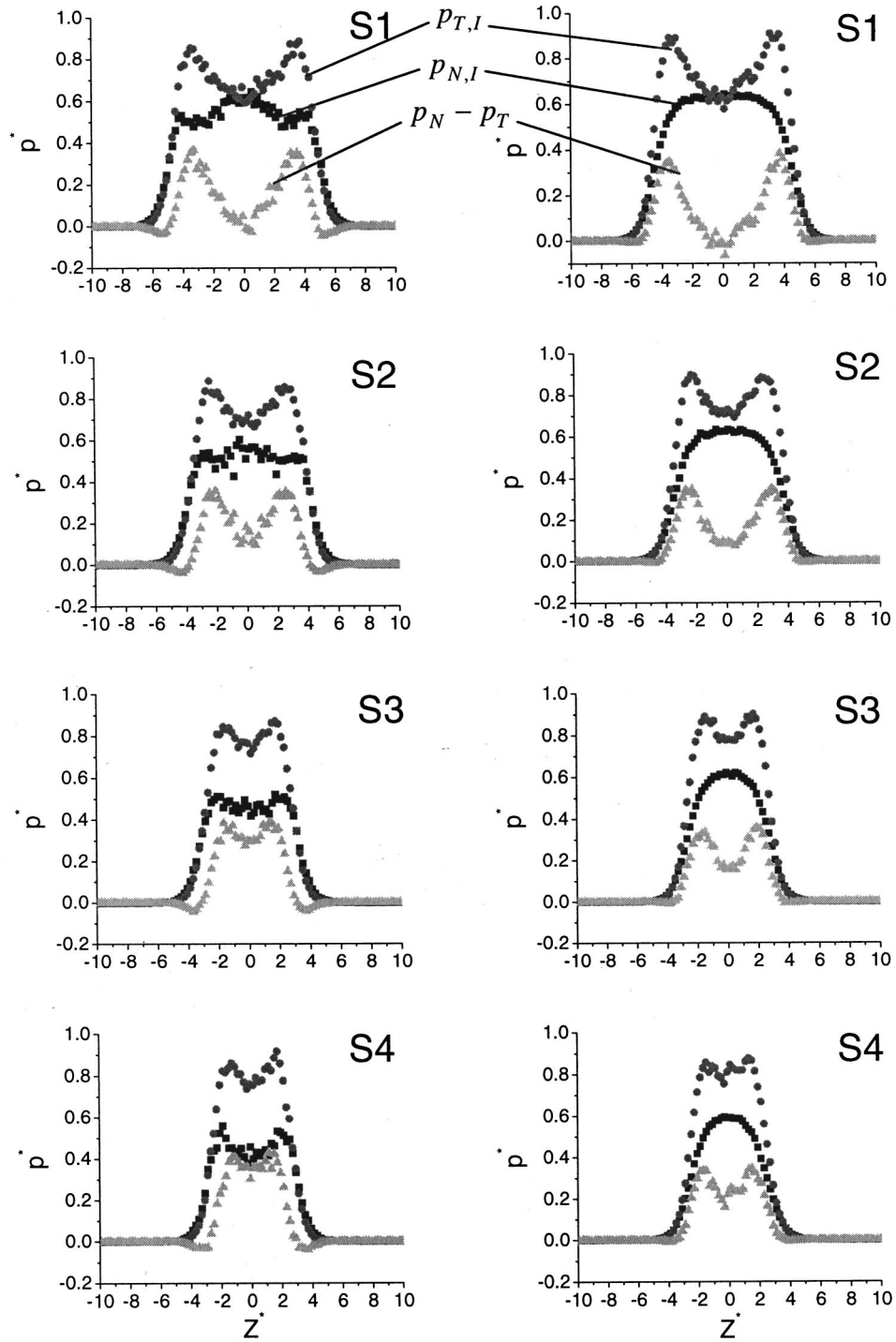

FIG. 5. Profiles of inertial parts of local normal pressure $p^*_{N,I}$ (■), inertial parts of local tangential pressure $p^*_{T,I}$ (●), and local stress $p^*_N - p^*_T$ (▲). The left column is from the simplified method and the right column is from the modified method.

to 1, while for the liquid phase, the liquid argon properties are used and ε_2 and n_2 are 1.4718 and 1.233 at $T^*=0.818$ (or $T=99$ K), respectively.[14] Typically, ν_e is about 3×10^{15} s^{-1} for various materials.[13] From Eq. (12), the Hamaker constant A at $T^*=0.818$ is about 2.01×10^{-20} J.

The total energy change $(\Delta W_s+\Delta W_\nu)$ should be positive for the film to be stable, that is, the wavelength should be smaller than the critical length,

$$\lambda<\lambda_{cr}=L_f^2\sqrt{\frac{4\pi^3\gamma_{l\nu}}{A}}, \tag{13}$$

For $L_f=5.03\sigma$ (S4) the critical wavelength λ_{cr} is 47.8σ. Due to the periodic boundary condition assumption, L_x can be understood as the longest wavelength allowed by the computation domain. According to this model, if $\lambda_{cr}\leqslant L_x$, a film may become unstable. For the same film at a higher temperature, since the surface tension $\gamma_{l\nu}$ decreases and λ_{cr} becomes smaller, the film will be less stable.

The simulation results in Table I show that, for a film with $L_f=5.03\sigma$, $L_x=17.1\sigma$ is the stable condition (S4) while increasing L_x to 20.52σ destroys the film (L2). This seems to indicate that the value of the critical wavelength λ_{cr}

Downloaded 04 Sep 2005 to 165.123.34.86. Redistribution subject to AIP license or copyright, see http://jcp.aip.org/jcp/copyright.jsp

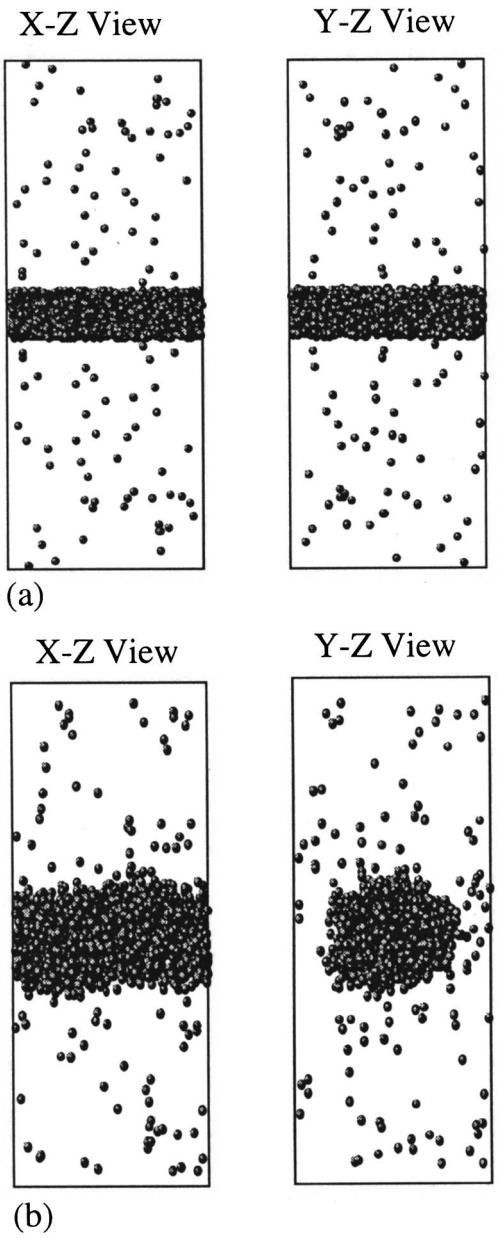

FIG. 6. Snapshot of (a) initial position of molecules (initial film thickness $L_s^* = 4.28$) and (b) final position of molecules after 160 000 steps.

is somewhere between 17.1σ and 20.52σ. There are several possible reasons for the difference between the results predicted by the classical thermodynamic model and MD simulation. First, the definition of film thickness is highly ambiguous. The classical approach assumes a zero-thickness interface and a well-defined film thickness, while MD shows that for a very thin film, the interface thickness is on the same order as the ''bulk'' film thickness. Secondly, the classical model treats one dimensional wave, while in this MD simulation, a wave in the y direction also exists which may further destabilize the film. Thirdly, the main electronic absorption frequency is not an exact value.

In addition to the surface wave argument, it might also be reasonable to assume that the film becomes unstable because its center cannot sustain the large tensile stress in its metastable state. For a film with the same thickness but different crosssectional area, the center liquid density and local stress distribution are the same. But the perturbation (not necessarily the surface wave) depends on the cross-sectional area of the computational domain. The film with the larger cross-sectional area is less stable due to the increased perturbation. Similarly, perturbation is intensified at higher temperatures, which explains why increasing temperature will destabilize the film.

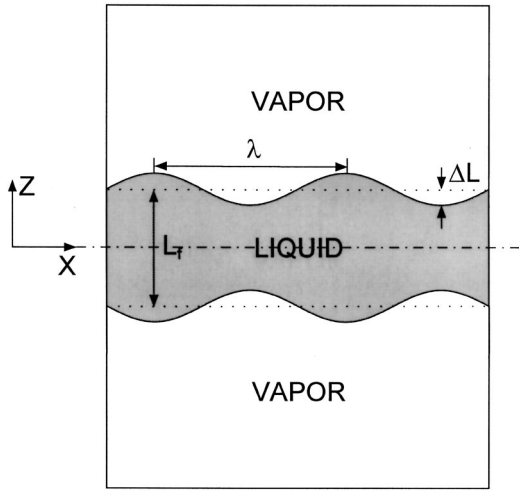

FIG. 7. Perturbation of a free liquid film suspended in its vapor.

When rupture occurs, the center liquid will release the stress. It can be expected that if the liquid is under larger stress (i.e., if the film is thinner), the rupture rate will be higher. However, the film thickness effect on the rupture rate has not been carefully investigated. The exact location where rupture initiates is also unknown.

VI. CONCLUDING REMARKS

This work studies the film thickness effect on interfacial properties. It is found that as the film thickness decreases, the two interfacial regions begin to overlap, which increases the local stress at the center of the film. As the local stress exceeds the maximum value, film rupture occurs. An improved method is proposed and found to be able to yield a more accurate profile of the normal pressure component, which indicates that it can obtain a better estimation on local stress as well. A macroscopic thermodynamic analysis is developed to study stability of the free film. Since it is still questionable whether macroscopic theories can be directly applied to such a thin film, the results between the thermodynamic model and the MD simulation cannot be quantitatively compared.

It is also important to study the film stability of a film on the solid substrate or a film between two solid plates, since these two cases are frequently encountered in industrial applications, such as spread wetting and phase-change cooling. A detailed investigation on the local stress profile and film stability may reveal some new understanding on wetting coefficients and disjoining pressures.

Downloaded 04 Sep 2005 to 165.123.34.86. Redistribution subject to AIP license or copyright, see http://jcp.aip.org/jcp/copyright.jsp

ACKNOWLEDGMENTS

The authors gratefully acknowledge financial support from the U.S. Department of Energy and the National Science Foundation. Seungho Park has been partially supported for this research by grants from the Korea Science and Engineering Foundation under Contract No. 1999-1-304-002-5.

[1] O. D. Velev, T. D. Gurkov, I. B. Ivanov, and R. P. Borwankar, Phys. Rev. Lett. **75**, 264 (1995).
[2] G. A. Chapela, G. Saville, S. M. Thompson, and J. S. Rowlinson, J. Chem. Soc., Faraday Trans. 2 **73**, 1133 (1977).
[3] M. J. P. Nijmeijer, A. F. Bakker, C. Bruin, and J. H. Sikkenk, J. Chem. Phys. **89**, 3789 (1988).
[4] H. Daiguji and E. Hihara, Heat and Mass Transfer **35**, 213 (1999). Reference 4 can be found at: http://link.springer-ny.com/link/service/journals/00231/bibs/9035003/90350213.htm
[5] M. Mecke, J. Winkelmann, and J. Fischer, J. Chem. Phys. **107**, 9264 (1997).
[6] C.-C. Hwang, J.-Y. Hsieh, K.-H. Chang, and J.-J. Liao, Physica A **256**, 333 (1998).
[7] M. P. Allen and D. J. Tildesley, *Computer Simulation of Liquids* (Oxford University Press, New York, 1987).
[8] N. B. Vargaftik, *Table on the Thermophysical Properties of Liquids and Gases* (Hemisphere, Washington, D.C., 1975), p. 543.
[9] L.-J. Chen, J. Chem. Phys. **103**, 10214 (1995).
[10] J. S. Rowlinson and B. Widom, *Molecular Theory of Capillarity* (Clarendon, Oxford, 1982), Chap. 4, pp. 69–128.
[11] D. A. Edwards, H. Brenner, and D. T. Wasan, *Interfacial Transport Processes and Rheology* (Butterworth-Heinemann, Boston, MA, 1991), Chap. 12, pp. 305–322.
[12] A. Majumdar and I. Mezic, Microscale Thermophys. Eng. **2**, 203 (1998).
[13] J. Israelachvili, *Intermolecular and Surface Forces* (Academic, London, 1992), Chap. 11, pp. 176–212.
[14] *Numerical Data and Functional Relationships in Science and Technology, Vol. 6-II/8, Landolt–Bornstein* (Springer, New York, 1962); *Vol. IV/6, Landolt–Bornstein* (Springer, New York, 1982).

Downloaded 04 Sep 2005 to 165.123.34.86. Redistribution subject to AIP license or copyright, see http://jcp.aip.org/jcp/copyright.jsp